Military Technical College
Kobry El-Kobbah
Cairo, Egypt

10th International Conference
On Aerospace Sciences&
Aviation Technology

THREE-DIMENSIONAL BOUNDARY LAYER NEAR THE TIP OF HELICOPTER ROTOR

BY

Mohamed A. Elsharnoby*

ABSTRACT

The three-dimensional viscous flow near the rotor tip is one of the most important and difficult problems in rotor dynamics. Most of theoretical investigations focused upon the tip flow field problem confined to inviscid analysis. The detailed study of the complex three-dimensional viscous flow near the tip region can play an important role in determining the generated rotor noise, rotor performances, and dynamic loading of the rotor blade.

Through solving the boundary layer flow, the present work is to deeply investigate the viscous flow near the rotor tip. The solution of the boundary layer flow at that region is expected to explain many phenomena that arise in rotor dynamic.

KEY WORDS

Three-Dimensional Boundary Layer, Viscous Flow Around Helicopter Rotor Tip, Rotor Performance.

* Assist Prof.' Mechanical Engineering Department, Benha High Institute of Technology, Benha- Egypt.

INTRODUCTION

The three-dimensional viscous flow field near the helicopter rotor tip is one of the most complex and important problem in modern helicopter aerodynamics. As stated by Conlisk[1] " the flow generated by a helicopter is extremely complicated and difficult to measure, model, and predict." Conlisk gives a complete overview of the fundamentals of the helicopter aerodynamics in all flight regimes (hover, forward, etc). He also discusses the formation of the tip vortex and the associated rotor wake. The formation of the tip vortex and the structure of the rotor wake is also analyzed by Li [2] who applied the vortex lattice method to predict accurately the vortex rollup in the vicinity of the rotor tip.

Lin et al [3} have reviewed some of the analytic approaches to the problem of tip vortex generation. Some of these solutions are based upon inviscid formulations. They give more accurate numerical solution of the viscous flow at the rotor tip assuming both laminar and turbulent boundary layer flows. A three-dimensional, forward marching, viscous flow analysis is applied to the tip vortex generation problem by Shamroth and Briley [4].

In this paper we shall consider one of the complex fluid dynamic problems associated with helicopter rotor. Several important features of viscous boundary layer on helicopter rotor have been demonstrated. The primary focus of this work is to study and compute the velocity distributions inside the boundary layer near the tip of helicopter rotor.

THE INVISCID FLOW SOLUTION

For solving the boundary layer equations, the inviscid flow velocity components outside the boundary layer are needed to stand for the boundary values of the velocity outside the boundary layer. To obtain the chord wise velocity component U and the span wise velocity component V for the inviscid flow, the rotor blade is modeled by horseshoe-vortex panels (Fig.1), as described by Li[2]

The panel circulations are calculated such that the normal velocity at collocation points set to be zero. From circulation distributions, the inviscid velocity components U and V are calculated assuming zero circulation at the trailing edge. The velocity components U, V are put as boundary values when solving the boundary layer equation.

THE BOUNDARY-LAYER EQUATIONS

The derivation of the boundary-layer equations near the rotor tip is starts by assuming the form of these equations in generalized rotating coordinates given by Mager[5]. After some mathematical manipulations, the boundary layer equations in Cartesian coordinates have the following dimensionless form,

$$\frac{\partial u}{\partial x}+\frac{\partial v}{\partial y}+\frac{\partial w}{\partial z}=0 \qquad \text{continuity}$$

$$\frac{\partial u}{\partial t}+u\frac{\partial u}{\partial x}+v\frac{\partial u}{\partial y}+w\frac{\partial u}{\partial z}=-\frac{\partial p}{\partial x}+\frac{\partial^2 u}{\partial z^2} \qquad \text{x\_momentum}$$

$$\frac{\partial v}{\partial t}+u\frac{\partial v}{\partial x}+v\frac{\partial v}{\partial y}+w\frac{\partial v}{\partial z}=-\frac{\partial p}{\partial y}+\frac{\partial^2 v}{\partial z^2} \qquad \text{y\_momentum}$$

where z is the boundary layer coordinate normal to the surface, *x* is the chordwise coordinate and y is the inner variable in the spanwise direction as indicated by Li[2]. The origin of the coordinates coincides with the leading point of the rotor tip section, u, v, w are the velocity components in the x, y, z directions respectively, p is dimensionless pressure which replaces the static pressure divided by the dynamic pressure of the upstream flow at the rotor tip. The dimensionless variables in continuity, x_momentum and y_momentum equations are defined by:

$$x=\frac{x^*}{l},\ y=\frac{y^*}{c},\ z=\frac{z^*}{l}\sqrt{R_e},\ t=\frac{\omega l}{c}t^*$$

$$u=\frac{u^*}{\omega l},\ v=\frac{v^*}{\omega l},\ w=\frac{w^*}{\omega l}\sqrt{R_e},\ p=\frac{p^*}{\rho\omega^2 l^2}$$

The superscript * denotes dimensional variables, *l* is the rotor span, c is the rotor chord and ω is rotating speed of the rotor.
The continuity, x_momentum and y_momentum equations are subjected to the following boundary conditions:

At surface (z = 0)

u = v = w = 0 (no slip condition)

as $z \to \infty$

$$u = U,\ v = V \text{ and } \frac{\partial u}{\partial y}=\frac{\partial v}{\partial x}$$

where U and V are the inviscid velocity components in the x and y directions respectively. The normal coordinate z is replaced by Rayleigh variable defined by:

$$\eta=\frac{z}{2\sqrt{t}}$$

Also, to cluster the points near the wall where the flow is expected to vary rapidly,

$$\eta=\frac{2\xi}{1-\xi}$$

where ξ is the new normal coordinate and has range between 0 and 1. The continuity and momentum equations become

$$\frac{\partial u}{\partial x}+\frac{\partial v}{\partial y}+\xi_z\frac{\partial w}{\partial \xi}=0$$

$$\frac{\partial \vec{F}}{\partial t}+u\frac{\partial \vec{F}}{\partial x}+v\frac{\partial \vec{F}}{\partial y}+(\xi_t+u_r-\xi_{zz})\frac{\partial \vec{F}}{\partial \xi}-\xi_z{}^2\frac{\partial^2 \vec{F}}{\partial \xi^2}=-\vec{P}$$

where $\xi_t=\frac{\partial \xi}{\partial t}$, $\xi_z=\frac{\partial \xi}{\partial z}$, $\xi_{zz}=\frac{\partial^2 \xi}{\partial z^2}$, $-\vec{F}=(u,v)$ and the pressure gradient vector $\vec{P}=(\frac{\partial p}{\partial x},\frac{\partial p}{\partial y})$.

The pressure gradient vector $\vec{P}$ is calculated using the inviscid surface speeds obtained from the panel code.

The problem started by assuming parabolic velocity distributions inside the boundary layer for both u and v. These distributions, to satisfy the boundary conditions, have zero values at the wall and reach asymptotically the values of inviscid velocity at the boundary layer edge ξ_{max}. These distributions will be our numerical initial conditions for the solution of the boundary layer equations.

GRID DISTRIBUTION AND NUMERICAL SOLUTION

While the grids are distributed uniformly in the chordwise directions, there is a cluster of grids near the rotor tip to measure the rapid variations of inviscid flow variables there. The spanwise distribution of panels used by Li[2] was adopted here to evaluate the panels circulations. The rotor blade is divided into two region the inner region and outer region as shown in Figure 1. The numerical solution contains two major steps; the first one solves the inviscid flow; and the second solves the boundary-layer equations.

The vortex panel method applied to rotating wing was used to get the inviscid flow solution around the helicopter rotor. The panels on the rotor surface are modeled by horseshoe vortices (Fig.2). For inviscid flow solution, the source Fortran program of Li was used to obtain the vorticity distribution on the surface at rotor tip. Some modifications on the program are made to sustain zero vorticity at the trailing edge. Also a part is added to evaluate beside the induced velocities at collocation points.

The uniform flow velocity is added to the induced velocity to obtain the velocity components U and V outside the boundary layer. Once the outer flow velocity components are known at collocation points, we assume parabolic distributions of velocities inside the boundary layer. These assumed distributions satisfy the non-slip condition of u and v at the wall and approach the values of U and V at the edge of the boundary layer. These distributions are put as initial values to the program that solving the boundary layer equations.

For solving the boundary-layer equations, the same technique of Xiao et all [6] is used. The Fortran program of Xiao [7] was modified to solve the boundary-layer equations assuming fixed grids. The pressure gradients included in the boundary layer equation are computed from the inviscid flow solution.

The Crank-Nicholson method is used to obtain the time derivatives in the equations. Also, the spatial derivatives are evaluated using the standard central difference operator. Different time steps were used in solving the equations; and it was observed that the smaller is the time step Δt the faster is the convergence of the solution. The standard central differences replace the spatial derivatives in the equations.

RESULTS AND DISCUSSIONS

Figure 3 shows the vorticity distribution over a rotating blade at angle of attack of 12°. This distribution is obtained using the standard vortex panel method. The distribution shows that vortex intensity increases towards the trailing edge of the rotor and also becomes greater far from the tip region of the helicopter rotor. The surface integration of vorticity results in the spanwise circulation distribution at the trailing edge shown in Fig.4.

When solving the boundary-layer equations, the results are obtained for Blasius boundary layer by assuming the inviscid flow velocity in the chordwise direction U equals unity and zero value of V at all the collocation points. The results show that, at certain given time, the u-velocity has similar distributions at all points along the span for at forty percent of the chord (Fig.5). Figure 5 confirms also that the outer flow chordwise velocity component U increases when going away from the rotor tip. While Figure 6 shows the effect of time on u-velocity profile at leading edge of the rotor tip section, Figure 7 shows the same effect on the u-velocity at leading edge and forty percent of the chord of the rotor tip section. In Figure 8 one can see the both effects of time and spanwise location on the u-velocity. While the spanwise location remarkably affects on U , the time has only effect on u-velocity profile inside the boundary layer. Figures 6,7 and 8 confirm that the Blasius velocity profile will change from time to time as the normal coordinate is a time dependant. Because the normal coordinate is inversely proportional to the square root of time, shrinking of the boundary-layer thickness with time occurs.

For the blade rotating at angle of attack of 12°, the distribution of both u and v velocities inside boundary layer at different locations are presented in Figures 9, 10, and 11. Figures 9 and 10 show respectively the variation in the chordwise and spanwise velocity components, u and v, when moving in the chordwise direction. Both Figures indicate that moving in chordwise direction results in similar effect in increasing both u and v. While the outer flow velocity U increases when moving far from the tip of the rotor (Fig.5), on the contrary, Figure 11 indicates that V has its extreme values at the tip section The effect of spanwise location on spanwise velocity v is quite similar to that concluded from Figure 12 of velocity vector near the rotor tip given by Lin[3]. Both results indicate that v has its maximum values at that region of the rotor tip.

CONCLUSIONS

From the numerical solution and the outcoming results, one concludes the following:
- The solution of the equations in that problem is reached faster for smaller time step.
-The inviscid Velocity distributions are as expected (do make sense).
-With time marching implicit technique, more stable solution is reached faster.
-The boundary layer becomes thinner with increasing time.
-The results compare well for the spanwise velocity variation along the span.

REFERENCES

1. Conlisk, A. T. : Modern Helicopter Aerodynamics. Annu. Rev. Fluid Mech. Vol. 29, pp 515-567, 1997.
2. Li, H. :The formation of rotor tip vortices. M. Sc. Thesis, Ohio State University 2000.
3.Lin, S. J., Levy, R., Shamroth, S. J., and Govindan T. R. : A Three-Dimensional Viscous Flow Analysis for the Helicopter Tip Vortex Generation Problem. NASA Contractor Report 3906, 1985.
4. R., Shamroth, S. J., and Briley, W. R.: A Viscous Flow Analysis for the Tip Vortex Generation Process. NASA Contractor Report 3906, 1979.
5. Mager, A.: Three-dimensional laminar boundary layers. Princeton University Series. High Speed Aerodynamics and Jet Propulsion. Princeton University Press. Vol. Iv ,pp. 286-394 ,1964.
6. Xiao, Z., Burggraf, O. R. & Conlisk, A. T. : The interacting boundary-layer flow due to vortex approaching a cylinder. J. Fluid Mech, vol. 346, pp. 319-343, 1997.
7. .Xiao, Z. The Interacting Boundary-Layer Flow Due to Vortex Approaching a Cylinder. Ph. D. Dissertation, Ohio State University 1998.

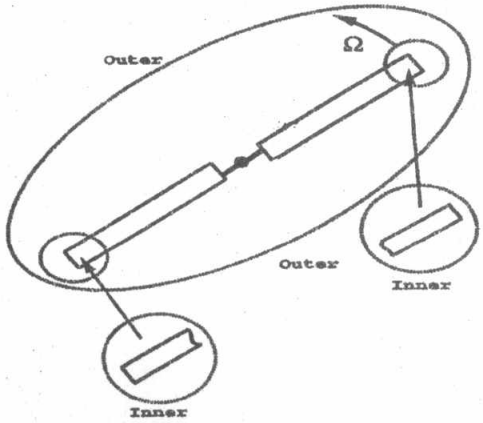

Fig.1 Definition of the inner and outer regions
for the calculation of the flow past a two-blade rotor

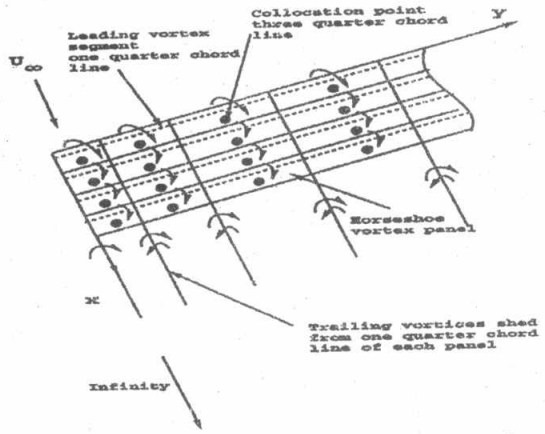

Fig.2 Horseshoe vortex model in the inner region

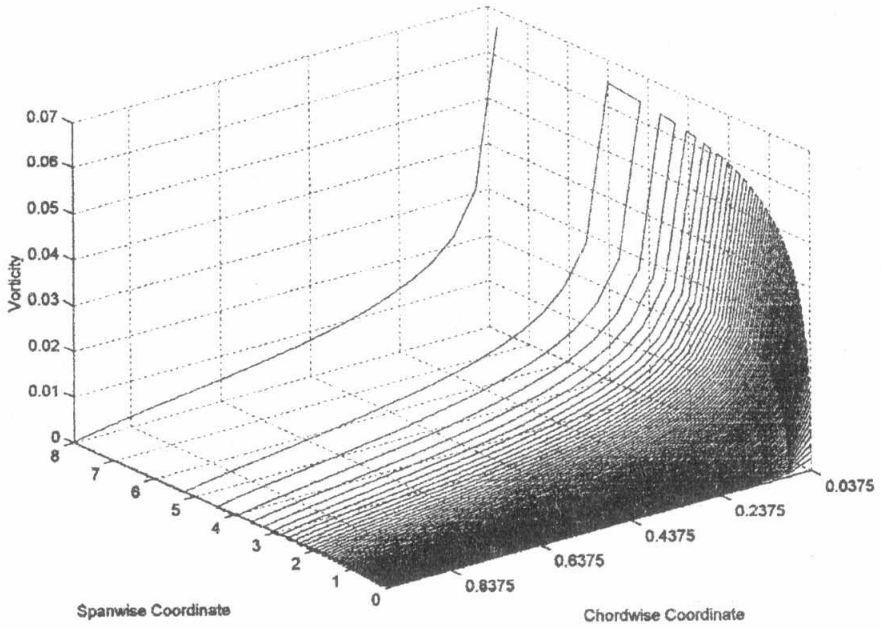

Fig.3 Vorticity distribution over the rotor blade surface near the tip

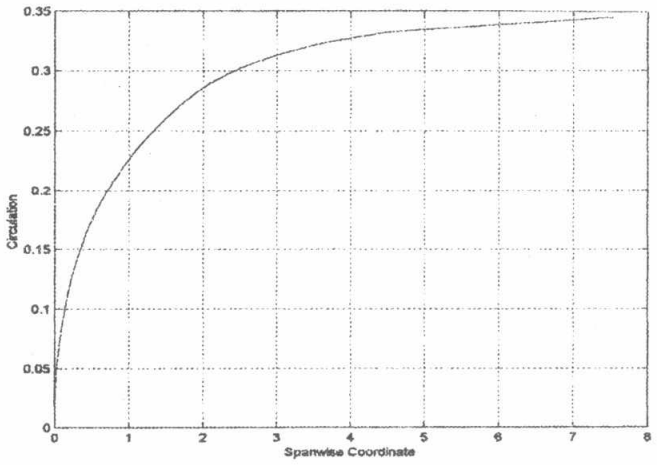

Fig.4 Total circulation along the trailing edge of the rotor blade

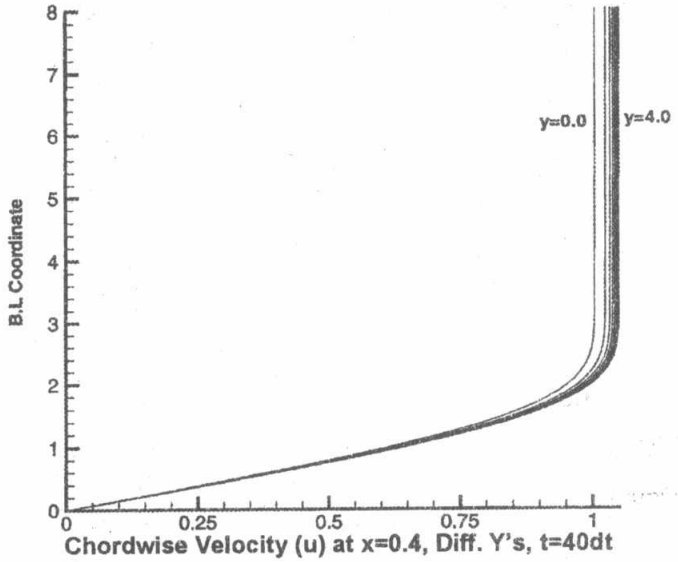

Fig.5 Similar profiles of the u-velocity at different locations

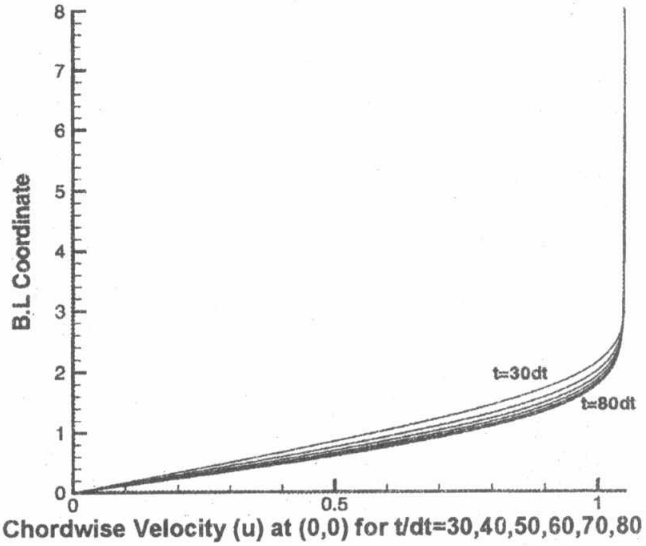

Figure 6 Effect of time on the u-velocity at the leading edge of the tip section

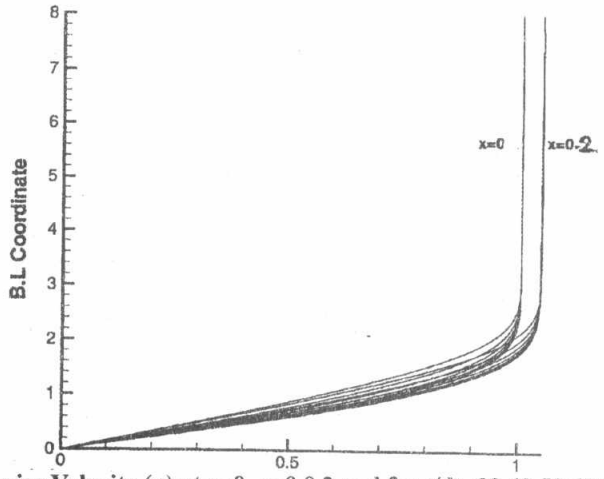

Chordwise Velocity (u) at y=0, x=0,0.2 and for t/dt=30,40,50,60,70,80

Figure 7 Effect of time and chordwise location on u-velocity

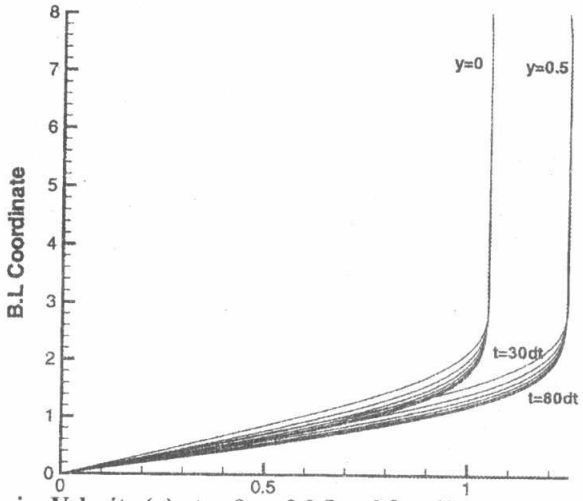

Chordwise Velocity (u) at x=0, y=0,0.5 and for t/dt=30,40,50,60,70,80

Fig.8 Effect of time and spanwise location on the u-velocity component

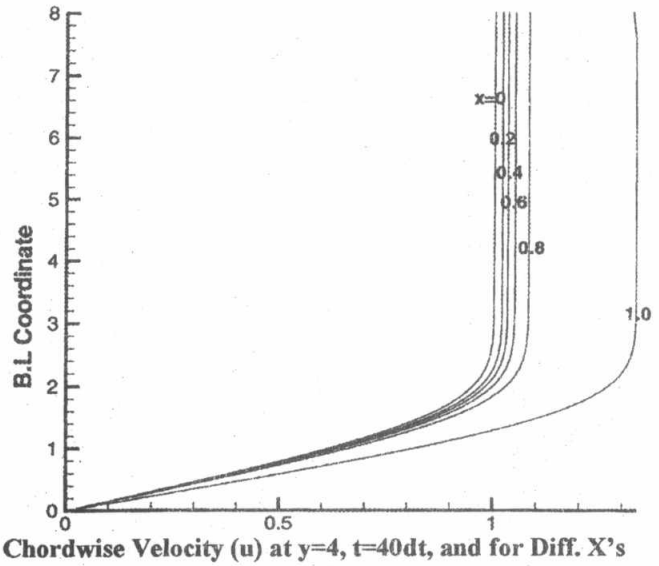

Fig.9 Effect of the chordwise location on the u-velocity component

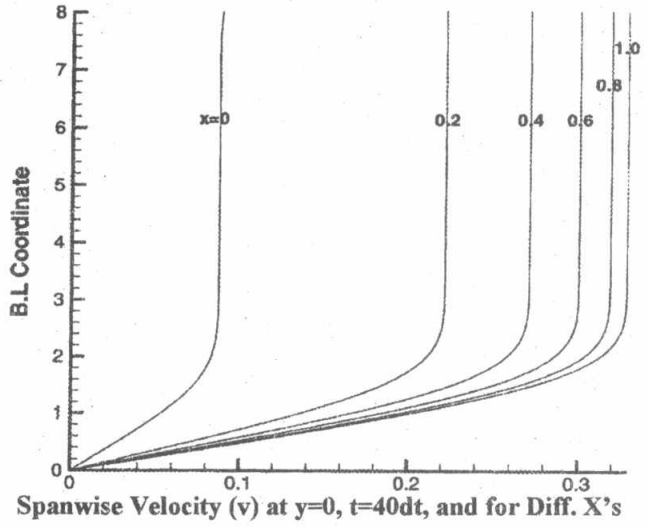

Figure 10 Effect of chordwise location on the v-velocity component

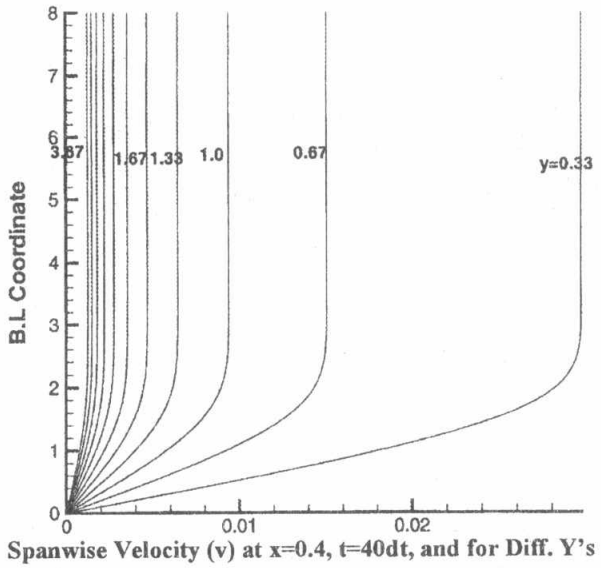

Figure 11 Effect of the spanwise location on the v-velocity component

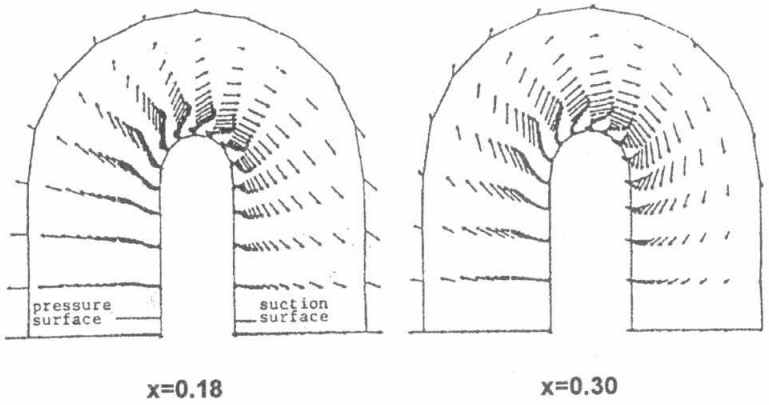

Fig.12 Velocity vector at the rotor tip (from ref.3)